Available online at www.sciencedirect.com

ScienceDirect

Ceramics International 40 (2014) 1661–1666

CERAMICS INTERNATIONAL

www.elsevier.com/locate/ceramint

Effects of ethyl cellulose polymers on rheological properties of (La,Sr)(Ti,Fe)O_3-terpineol pastes for screen printing

Setsuaki Murakami[a], Kinki Ri[a], Toshio Itoh[a], Noriya Izu[a], Woosuck Shin[a,*], Koji Inukai[b], Yosuke Takahashi[b], Yasunori Ando[b]

[a]*Electroceramics Processing Research Group, AIST, Nagoya 463-8560, Japan*
[b]*R&D Center, Noritake Co., Limited, Miyoshi 470-0293, Japan*

Received 27 June 2013; received in revised form 11 July 2013; accepted 11 July 2013
Available online 19 July 2013

Abstract

Ethyl cellulose (EC) was mixed with terpineol and conductive ceramic $La_{0.6}Sr_{0.4}Ti_{0.3}Fe_{0.7}O_{3-\delta}$ to prepare pastes with different EC content. Viscosity of the vehicles was found to increase with EC content, and the intrinsic viscosity, hydrodynamic radius, and effective sphere of EC in terpineol were estimated to be 0.07 L/g, 78.8 nm, and 0.06 L/g, respectively. For a ceramic paste of 70 wt% powder and vehicle, shear thinning properties were observed for pastes of 0 and 1 wt% EC. For EC contents above 3 wt%, the pastes become Newtonian-like behavior and EC was considered to act effectively as a dispersant. Screen printing of the pastes was carried out. The relative densities of the sintered films were as low as 51.7% for the 0 wt% EC paste, but increased to 67.6% for the 3 wt% EC paste. The high density observed for the 3 wt% EC paste was due to particles being well dispersed, which was also expected from the rheological results.

Keywords: A. Suspensions; D. Perovskites; E. Fuel cells; Rheology

1. Introduction

In recent years, solid oxide fuel cells (SOFCs), which can convert chemical energy into electrical energy directly, have been attracting considerable attention because of their high efficiency, low pollution, and fuel flexibility [1,2]. In previous research, we prepared a $La_{1-x}Sr_xTi_{1-y}Fe_yO_{3-\delta}$ (LSTF) material for use in oxygen permeable membrane reactors and found that a high ionic conductivity was obtained for a composition of $La_{0.6}Sr_{0.4}Ti_{0.1}Fe_{0.9}O_{3-\delta}$ [3,4]. This LSTF material can be applied as a cathode material for a SOFC, and we have since been trying to prepare screen-printed films of an SOFC electrolyte using the LSTF material.

To successfully prepare screen-printed films without defects or pinholes, it is important to control the rheological behavior of the paste. Similarly, the dispersibility of the ceramic powder and the stability of the dispersible particles in combination with a high ceramic powder content in the liquid phase (vehicle) are also very important factors. Generally, various organic additives such as a dispersant and a binder are added to formulate the paste for screen printing. The binder is a significant additive in preparing screen-printed films of high density without defects or pinholes, because the binder affects the viscoelastic property of the paste and the green film properties such as the strength, density, and inner structure of the film. When the binder content in the paste is too low, the green film cannot maintain the printed structure and develops cracks during drying as a result of the reduced network strength between the ceramic particles. On the other hand, when the binder content is too high, the viscosity of the paste increases and screen printing becomes difficult. Furthermore, the film thickness increases and the film density decreases after sintering [5].

Ceramic pastes based on ethyl cellulose (EC) as the binder and terpineol as an organic solvent have already been used for screen printing [1,5–8]. However, the details of the interaction between the ceramic powder and EC remain unclear [5,8]. We have reported on the viscoelastic properties of ceramic catalyst pastes for vehicles based on EC and terpineol [6]. In our previous report, we described how the EC plays two distinct roles by aiding dispersion of the ceramic particles and increasing the viscosity of

*Corresponding author. Tel./fax: +81 52 736 7107.
E-mail address: w.shin@aist.go.jp (W. Shin).

0272-8842/$ - see front matter © 2013 Elsevier Ltd and Techna Group S.r.l. All rights reserved.
http://dx.doi.org/10.1016/j.ceramint.2013.07.057

the paste. It is considered that the interactions between the ceramic catalyst particles and the EC are a key factor in successfully preparing screen-printed films without defects or pinholes. However, in our previous report we did not discuss the influence of the EC content in the paste on the screen-printed films.

In this paper, we report on the influence of the EC content in the paste on the rheological behavior of the pastes and on the thickness and relative density of the screen-printed films. To investigate the rheological behavior, pastes of different EC contents were prepared by mixing with terpineol and the LSTF powder. After describing the results of viscoelastic measurements of the pastes, we discuss the results in terms of the interaction between the LSTF powder and the EC. Furthermore, using these pastes, screen-printed films were prepared and the influence of the EC content in the paste investigated.

2. Experimental method

2.1. Preparation of $La_{0.6}Sr_{0.4}Ti_{0.3}Fe_{0.7}O_{3-\delta}$ (LSTF) paste

Powders of La_2O_3 (Wako Pure Chemical Industries, Ltd., grain size 1 μm), $SrCO_3$ (Wako, grain size 1 μm), TiO_2 (Wako, grain size 1 μm), and Fe_2O_3 (Wako, grain size 1 μm) were mixed to prepare various LSTF compositions. The powders were mixed using a ball mill with yttria stabilized ZrO_2 (YSZ) balls for 5 h, and then calcined at 1400 °C for 6 h. After calcination, the sample was milled by ball milling. Fig. 1 shows (a) the particle size distribution and (b) an SEM micrograph of the LSTF powder starting material. The average particle size ($D=0.5$) of the LSTF particles was 0.93 μm and the particle size distribution was fairly uniform. As shown in Fig. 1(b), the LSTF particles were of irregular shape. The specific surface area of the powder was 4.8 m^2/g.

A series of vehicles comprising the LSTF particles with EC (ethoxy content of about 50% and an average molecular weight of about 44000.) were prepared for EC contents from 0.1 wt% to 20 wt% with terpineol as an organic solvent (64 mPa·s) using a hybrid mixer (ARE310, Thinky, Japan). The vehicles and LSTF powder of 70 wt% were mixed into pastes by a roll-mill (EXAKT M-50, Nagase Screen Printing Research Co., Japan) at room temperature. The various compositions of the pastes are summarized in Table 1.

2.2. Rheological analysis of vehicles and pastes

The flow behavior of the vehicles and pastes was analyzed by a rheometer (MARS-2, HAAKE, Germany). Cone-plate (diameter=35 mm, $\phi=1°$) and parallel-plate (diameter=35 mm) geometries were used. Flow curves of the vehicles and pastes of different EC contents were measured at shear rates from 0.1 s^{-1} to 1000 s^{-1} at room temperature. After approach of the plate to the gap, any excess vehicle or paste squeezed out was wiped off. For the cone-plate geometry, the gap between the plate and the bottom of the measurement vessel was 0.005 mm, and for the parallel plate geometry, the gap was 0.1 mm.

Dynamic viscoelasticity measurements of the pastes were performed by the oscillation method using a parallel-plate (35 mm diameter) with a gap of 0.1 mm. Storage modulus (G') and loss modulus (G'') were measured at shear stress values from 0.1 to 1000 Pa at a frequency of 1.0 Hz at 25 °C, known as stress sweep measurements.

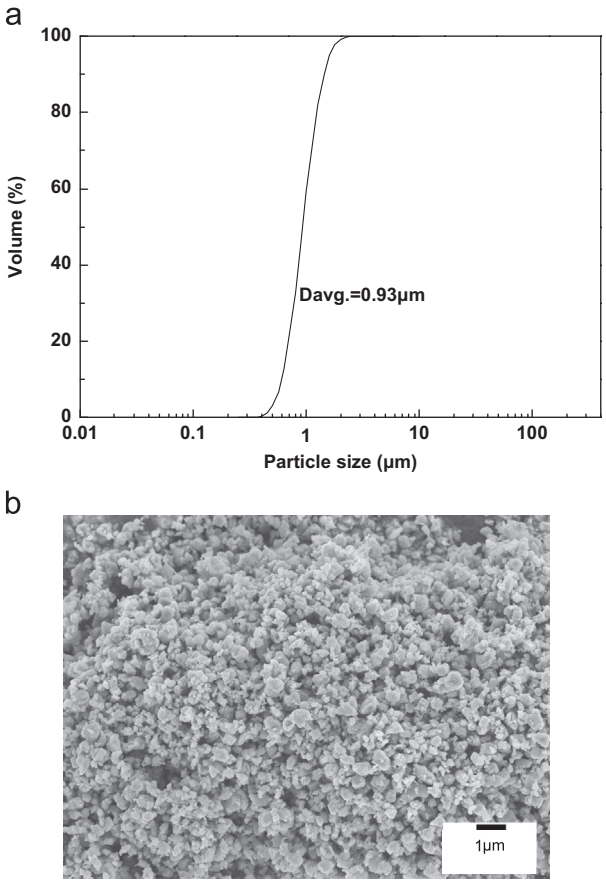

Fig. 1. (a) Particle size distribution and (b) SEM micrograph of the LSTF powder starting material.

2.3. Amount of adsorbed ethyl cellulose on LSTF

We analyzed the amount of adsorbed EC on the surface of the LSTF particles. The pastes were centrifuged at 18000 rpm at room temperature for 1 h to separate the sediment and the supernatant liquid in the pastes. The sediment was then washed with terpineol and dried in a vacuum oven at 95 °C for 16 h. The amount of EC adsorbed on the surface of the particles was estimated by the weight loss exhibited in the sediment under TG-DTA analysis (MTC1000SA, BRUKER, Japan). The sediment was heated from 25 to 500 °C at a heating rate of 5 °C/min in an air atmosphere. The amount of EC adsorbed on the surface of the LSTF particles was calculated by subtracting the weight loss of the sediment without EC (T-70) from the weight loss of the sediment of the EC pastes.

2.4. Screen-printed films

Pastes were printed onto silicon wafer substrates using a screen printer (LS-150, Newlong Seimitsu Kogyo, Japan). Screen printing was performed at a print speed of 30 mm/s and

Table 1
LSTF pastes with ethyl cellulose (EC) and terpineol. TG-weight loss of the sediments from 25 to 500 °C and shrinkages of the screen-printed films after sintering at 1000 °C for 1 h are also listed.

Sample	EC (wt%)	Terpineol (wt%)	LSTF powder (wt%)	TG-weight loss of sediment from 25 °C to 500 °C (%)	Shrinkage (%)
T-70	0.00	30.00	70	0.5	1.8
EC 1 wt%	0.30	29.70	70	0.6	14.1
EC 3 wt%	0.90	29.10	70	0.1	12.3
EC 5 wt%	1.50	28.50	70	0.9	11.8
EC 10 wt%	3.00	27.00	70	–	9.9
EC 15 wt%	4.50	25.50	70	–	7.7
EC 20 wt%	6.00	24.00	70	0.9	–

a screen of 200 mesh, a 0.1 mm snap-off distance, and 0.2 MPa of squeegee pressure. Green bodies of the screen-printed films were dried at 90 °C for 1 h, before heating at a rate of 5 °C/min to 1000 °C and sintering for 1 h. Four screen-printed film samples were prepared for every composition, as shown in Table 1.

The thickness of the screen printed films was measured by a contact film thickness measurement system (P-16+, KAL-Tencor, Japan). The surface of each screen printed film was observed using a field-emission scanning electron microscopy (JSM-6335FM, JEOL, Japan). For the FE-SEM observations, a thin coating of Pt was deposited on the surface of the pastes.

3. Results and discussion

Fig. 2(a) shows flow curves of the vehicles of different EC contents. Increasing the EC content in the vehicles led to an increase in their viscosity. In particular, the viscosities showed a rapid increase above 5 wt% EC and decreased at shear rates above 100 s^{-1}, indicating shear thinning behavior. To estimate the EC content at which interaction between the molecules occurs, an effective sphere model was used for measurements of dilute vehicles below 1 wt% EC.

The dependence of the relative viscosity, η_r ($\eta_r = \eta_s/\eta_1$, where η_s is the viscosity of the vehicle and η_1 is the viscosity of the organic solvent), of the vehicle on the concentration, C, was approximated by the equation

$$\eta_r = \exp(SC) \quad (1)$$

where S is the effective sphere of influence for the molecules [9]. S can be determined from the slope of [$\ln(\eta_r)$ vs. C], as $C \to 0$. Interaction between the molecules is observed as a departure from Eq. (1). S was 0.06 L/g and the viscosities of the vehicles of different EC contents were approximated by Eq. (1) (Fig. 2(b)). However, viscosities of the vehicles above 3 wt% EC departed from the approximated curve. This indicates that the EC in the vehicles below 2 wt% EC was present as isolated macromolecules, whereas the EC in the vehicles above 3 wt% EC overlapped and became entangled.

The behavior of isolated macromolecules of EC in the terpineol was estimated based on the intrinsic viscosity [η] and the hydrodynamic radius, R_H. Usually, the intrinsic viscosity

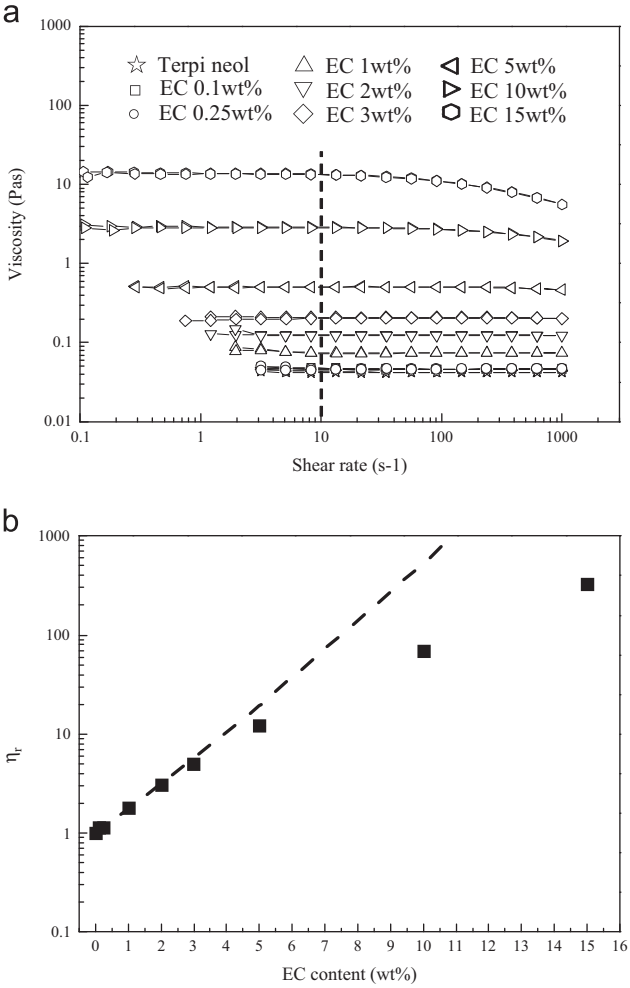

Fig. 2. (a) Flow curves of vehicles of different ethyl cellulose content and (b) relative viscosity at a shear rate of 10 s^{-1} with respect to ethyl cellulose content of vehicle. The dashed line indicates the curve fitted by the equation $\eta_s/\eta_L = \exp(SC)$. To obtain the effective sphere (S), the viscosities of dilute vehicles below 1 wt% EC were monitored at a shear rate of 10 s^{-1}, giving a value for S of 0.06 L/g.

[η] is defined as

$$[\eta] = \lim_{c \to 0} \frac{\ln \eta_r}{C} = \lim_{c \to 0} \frac{\eta_{sp}}{C} \quad (2)$$

where C is the concentration of EC and η_{sp} is the specific viscosity $\eta_{sp} = (\eta_s - \eta_L)/(\eta_L)\eta_{sp}$. The intrinsic viscosity [η] was determined from the intercept of [η_{sp}/C vs. C], as $C \to 0$.

Using Eq. (3), the R_H of a polymer in the solvent can be estimated based on the intrinsic viscosity [η] and molecular weight M [10]

$$[\eta] = 2.5\left(\frac{4\pi R_H^3 N_A}{3M}\right) \quad (3)$$

where N_A is Avogadro's number. Using the viscosities of vehicles below 1 wt% EC, the intrinsic viscosity [η] and R_H of an isolated macromolecule in the terpineol were estimated. The [η] and R_H values of EC in terpineol were 0.07 L/g and 78.8 nm, respectively. Hsu et al. reported that the [η] value for a vehicle of terpineol and EC (ethoxy content of about 50% and an average molecular weight of about 68000) was 0.12 L/g [11]. The [η] value of the present study was lower than that of Hsu et al. because of the lower average molecular weight (44000).

Fig. 3 shows (a) flow curves of the pastes of different EC contents, and (b) the viscosities of pastes and vehicles at a shear rate of 10 s^{-1}. Upon increasing shear rate, the viscosities of the pastes decreased and shear thinning behavior was observed in pastes of EC content below 1 wt%. This shear thinning became less pronounced with increasing EC content.

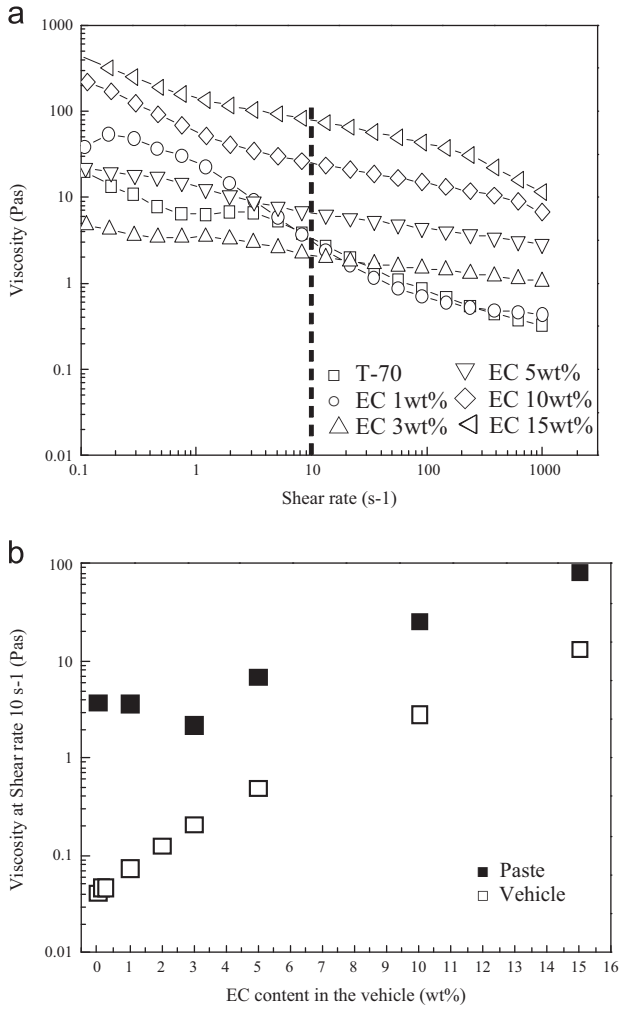

Fig. 3. (a) Flow curves of the pastes of different EC contents, and (b) viscosities of pastes and vehicles at a shear rate of 10 s^{-1}.

It seems that the LSTF particles in pastes above 3 wt% EC were well dispersed. The lowest viscosity among the pastes at 10 s^{-1} was observed for 3 wt% EC. Increasing the EC content of the pastes above 3 wt% increased the viscosity. This viscosity behavior for pastes above 3 wt% EC was similar to that observed for the vehicles. Overall, the rheological behavior of the pastes below 1 wt% EC depended on aggregation of the LSTF particles, whereas that of the pastes above 3 wt% EC depended on entanglement of the EC.

Fig. 4 shows the shear-stress dependence of the storage modules (G' of the pastes of different EC contents. G' and G'' are usually represented as

$$G^* = G' + iG'' \quad (4)$$

where $G'' = G^* \sin\delta$, and $G' = G^* \cos\delta$. When a viscoelastic fluid is characterized by the phase angle $0 < \delta < 90^\circ$, G′ is referred to as the elastic or storage modulus, which is a measure of the energy stored during the test, while G″ is the viscous or loss modulus, which is used to determine the energy for flow. In an ideal solid $G^* = G'$, whereas for an ideal liquid $G^* = G''$ [12,13].

The G' value of T-70 decreased rapidly at a shear stress of 6 Pa and crossover of G' and G'' was observed. It seems that aggregates of the LSTF particles in the paste collapsed under the shear stress [14]. The G' value of the pastes with EC was lower than the loss modules (G'') (i.e., $G' < G''$, data not shown). The G' values of the pastes increased with increasing EC content in the pastes.

The G' value of the paste of 1 wt% EC increased from a shear stress of 1 Pa and was maximum at a shear stress 10 Pa. An increase in G' was observed for the paste of 3 wt% EC, while with further increases in EC content, the increase in G' was reduced. Further increases in G' were not observed for the pastes of 5, 10, and 15 wt% EC. The particles in the pastes of 1 and 3 wt% EC reaggregated under the flow and G' consequently increased. For the pastes with increased EC content, reaggregation of the LSTF particles was inhibited due to entanglement of the EC.

Table 1 shows the TG weight loss of the sediments from 25 to 500 °C. The TG weight loss of T-70 was 0.5%, and this

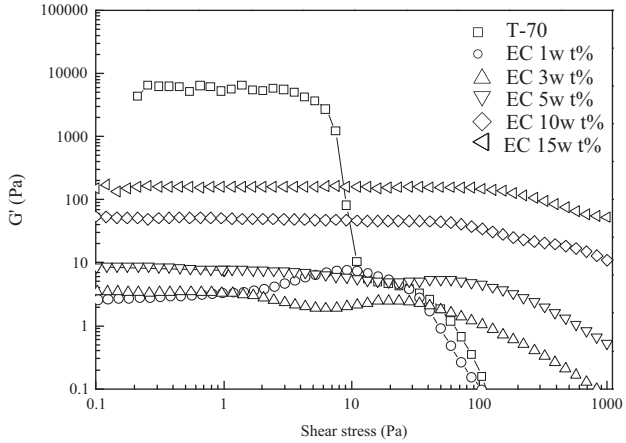

Fig. 4. Shear-stress dependence of the storage modules (G') of the pastes of different EC contents.

value was subtracted from the measured weight losses of the EC paste sediment to obtain the EC content in the sediments. The EC contents in the sediments were 0.1, 0.5, 0.4, and 0.4% for the 1, 3, 5, and 20 wt% EC pastes, respectively. If we consider the nominal composition taking, for example, the 1 wt % EC paste, we obtain a mixture of 75% of the EC as a free polymer with the remaining 25% EC either adsorbed or agglomerated on the particles. Furthermore, it seems that saturation absorption of EC on the surface of particle occurred over 3 wt% EC paste. From these results, we can conclude that the EC contributes to improvement of dispersion stability of particles. Presumably, at low EC content, the polymer chains hardly approach the surfaces of all individual particles because of high flocculated state.

By using the hydrodynamic radius of EC, the EC contents in the sediments and the specific surface area of the particles, EC weight per unit area of particle was calculated. In monolayer model EC weight per unit area of particle was 0.018 mg/m^2, whereas that of the pastes above 3 wt% EC was 0.83 mg/m^2. It seems that aggregates of EC were adsorbed on particles. However, it is generally known that the adsorbance of polymer on solid surfaces is of the order of 1 mg/m^2 because of loop conformation of adsorbed chain. It is also acceptable to understand the data above without aggregate formation of EC.

Fig. 5 shows the (a) thicknesses and (b) relative densities of the green films and sintered films as a function of EC content in the vehicle. The screen-printed films did not appear to show any pinholes or cracks under visual inspection visually. For EC contents up to 3 wt% the film thickness decreased, while for EC contents of 5 and 10 wt% the film thickness was increased,

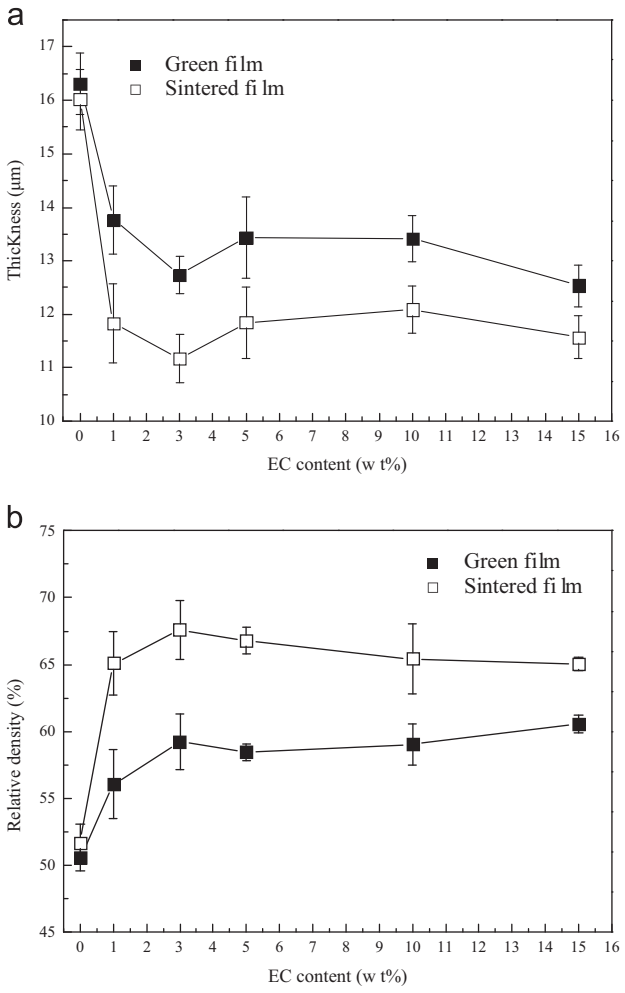

Fig. 5. (a) Thicknesses and (b) relative densities of green films and sintered films as a function of EC content in the vehicle.

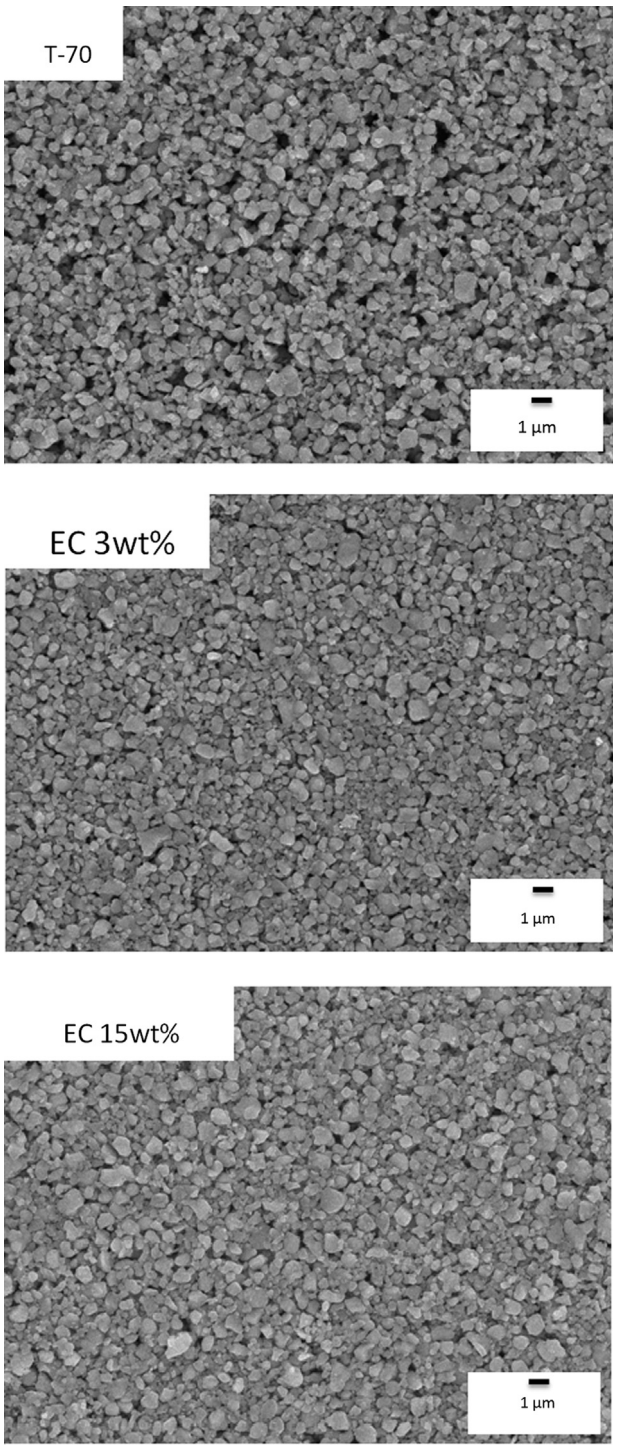

Fig. 6. SEM micrographs of surfaces of films of 0, 3, and 15 wt% EC after sintering at 1000 °C for 1 h.

with the 5 and 10 wt% EC samples having almost the same thickness. Furthermore, for an EC content of 15 wt%, the film thickness decreased. The initial decrease in thickness was caused by aggregation or reaggregation of LSTF particles in the pastes. Upon increasing the EC content, aggregation or reaggregation in the paste decreased and the resulting film thickness was reduced, reaching its lowest value for 3 wt% EC. The second decrease in the thickness at 15 wt% EC was caused by the high viscosity of the paste. Some of this high viscosity paste was observed on the screen mesh during lift up, such that the resulting thickness of the transferred film was low.

As shown in Table 1, the shrinkage ratio of the film thickness after sintering became smaller with increasing EC content. This was a reasonable result considering that the excess EC content enhances the pore structure, which leads to less densification.

After sintering at 1000 °C for 1 h, the relative densities of the films were obtained (Fig. 5(b)). Upon increasing the EC content up to 3 wt%, the film density increased to a maximum. For further increases in the EC content above 5 wt% the film relative density slightly decreased. Again, the increase in film relative density up to 3 wt% EC was caused by a decrease in aggregation or reaggregation of the LSTF particles in the pastes. The decrease in film relative density above 5 wt% EC was caused by excess EC impeding the sintering process. The changes in film relative densities were consistent with the observed shrinkage ratio (Table 1).

Fig. 6 shows SEM micrographs of the surfaces of films of 0, 3, and 15 wt% EC after sintering at 1000 °C for 1 h. The 0 wt % EC film showed many surface defects, but the other films were smooth. This is consistent with the observation of shear thinning behavior for the 0 wt% EC paste, in which agglomeration of the particles occurred. In contrast, the other pastes were well dispersed. The agglomeration of the 0 wt% EC paste resulted in defects in the film surface.

In summary, it was found that an EC content of 3 wt% was optimum for the pastes, which gave a screen-printed film with lower thickness and higher density.

4. Conclusion

A binder of ethyl cellulose (EC) was mixed with terpineol as an organic solvent and conductive ceramic powder of $La_{0.6}Sr_{0.4}Ti_{0.3}Fe_{0.7}O_{3-\delta}$ to prepare pastes of different EC contents.

The relative viscosity of the vehicles was found to increase with EC content, and the intrinsic viscosity, hydrodynamic radius (R_H) and the effective sphere of EC in terpineol were estimated to be 0.07 L/g, 78.8 nm, and 0.06 L/g, respectively. The increase in relative viscosity was exponential to 3 wt% EC, before increasing at a slower rate, and at high EC contents, agglomeration of EC seemed to occur.

For a ceramic paste comprised of 70 wt% powder and different vehicle compositions, shear thinning properties were observed for pastes of 0 and 1 wt% EC. For EC contents above 3 wt%, the pastes become Newtonian-like and EC was considered to act effectively as a dispersant. Screen printing using the pastes was carried out on the Si wafers before sintering at 1000 °C for 1 h. The relative densities of the sintered films were as low as 51.7% for the 0 wt% EC paste, but increased to 67.6% for the 3 wt% EC paste. The high relative density observed for the 3 wt% EC paste is due to the particles being well dispersed in the structure, which was also expected from the rheological results. For the films of high EC content, the relative density of the sintered film decreased slightly as the EC content was increased because of excess EC. Overall, an EC content of 3 wt% in the vehicle was found to be optimum, resulting in screen-printed films with lower thickness and higher density than the other films.

References

[1] Y. Zhang, X. Huang, Z. Lu, Z. Liu, X. Ge, J. Xu, X. Xin, X. Sha, W. Su, A screen-printed $Ce_{0.8}Sm_{0.2}O_{1.9}$ film solid oxide fuel cell with a $Ba_{0.5}Sr_{0.5}Co_{0.8}Fe_{0.2}O_{3-\delta}$ cathode, Journal of Power Sources 160 (2006) 1065–1070.

[2] N.T. Hart, N.P. Brandon, M.J. Day, J.E. Shemilt, Functionally graded cathodes for soid oxide fuel cells, Journal of Materials Science 36 (2001) 1077–1085.

[3] Y. Takahashi, T. Suzuki, A. Kawahara, Y. Ando, M. Hirano, W. Shin, Dilatometry and high-temperature X-ray diffractometry study of $La_{0.6}Sr_{0.4}Ti_{0.1}Fe_{0.9}O_{3-\delta}$ and $La_{0.6}Sr_{0.4}Ti_{0.3}Fe_{0.7}O_{3-\delta}$ oxygen-permeable membranes, Solid State Ionics 181 (2010) 1516–1520.

[4] Y. Takahashi, A. Kawahara, T. Suzuki, M. Hirano, W. Shin, Perovskite membrane of $La_{1-x}Sr_xTi_{1-y}Fe_yO_{3-\delta}$ for partial oxidation of methane to syngas, Solid State Ionics 181 (2010) 300–305.

[5] J.W. Phair, Rheological analysis of concentrated zirconia pastes with ethyl cellulose for screen printing SoFC electrolyte films, Journal of the American Ceramic Society 91 (2008) 2130–2137.

[6] W. Shin, M. Nishibori, M. Ohashi, N. Izu, T. Itoh, I. Matsubara, Ceramic catalyst combustors of Pt-loaded-alumina on microdevices, Journal of the Ceramic Society of Japan 117 (2009) 659–665.

[7] C.J. Hsu, J.H. Jean, Formulation and dipersion of NiCuZn ferrite paste, Materials Chemistry and Physics 78 (2002) 323–329.

[8] S. Lee, U. Paik, S.M. Yoon, J.Y. Choi, Dispersant-ethyl cellulose binder interaction at the Ni particle-dihydroterpineol interface, Journal of the American Ceramic Society 89 (2006) 3050–3055.

[9] J.S. Reed, Rheology of Saturated Systems (Slurries and Pastes) in Principles of Ceramics Processing, second ed., John Wiley and Sons, INC.289–290.

[10] M. Kawahigashi, H. Sumida, K. Yamamoto, Size and shape of soil humic acid estimated by viscosity and molecular weight, Journal of Colloid and Interface Science 284 (2005) 463–469.

[11] C.J. Hsu, J.H. Jean, Formulation and dispersion of NiCuZn ferrite paste, Materials Chemistry and Physics 78 (2002) 323–329.

[12] I. Santacruz, J. Binner, Rheological characterization and coagulation casting of Al_2O_3-nano zirconia suspensions, Journal of the American Ceramic Society 91 (2008) 33–40.

[13] S. Murakami, K Ri, T. Itoh, I. Izu, W. Shin, K. Inukai, Y. Takahashi, Y. Ando, Influence of particle size and aggregation state of alumina on the rheology of a ceramic paste with an organic binder of ethylene–vinyl acetate copolymer and stearic acid, Ceramics International 38 (2012) 1591–1597.

[14] T. Goto, Y. Otsubo, Rheology control of ceramic slurries for sintering of this films, Journal of the Society of Rheology Japan 29 (2001) 205–210.